Journal of Power Sources 196 (2011) 4987–4991

Contents lists available at ScienceDirect

Journal of Power Sources

journal homepage: www.elsevier.com/locate/jpowsour

$Sm_{0.2}(Ce_{1-x}Ti_x)_{0.8}O_{1.9}$ modified Ni–yttria-stabilized zirconia anode for direct methane fuel cell

Yu Chen[a,b], Fanglin Chen[b], Wendong Wang[c], Dong Ding[d], Jianfeng Gao[a,*]

[a] CAS Key Laboratory of Materials for Energy Conversion, Department of Materials Science and Engineering, University of Science and Technology of China, Hefei, 230026 Anhui, China
[b] Department of Mechanical Engineering, University of South Carolina, 300 Main Street, Columbia, SC 29208, USA
[c] Department of Chemical Physics, University of Science and Technology of China, Hefei 230026, China
[d] School of Materials Science and Engineering, Georgia Institute of Technology, Atlanta, GA 30332, USA

ARTICLE INFO

Article history:
Received 2 December 2010
Received in revised form 17 January 2011
Accepted 19 January 2011
Available online 26 January 2011

Keywords:
Solid oxide fuel cell
Impregnation
Doped ceria
Direct methane fuel cell

ABSTRACT

$Sm_{0.2}(Ce_{1-x}Ti_x)_{0.8}O_{1.9}$ (SCT*x*, $x = 0$–0.29) modified Ni–yttria-stabilized zirconia (YSZ) has been fabricated and evaluated as anode in solid oxide fuel cells for direct utilization of methane fuel. It has been found that both the amount of Ti-doping and the SCT*x* loading level in the anode have substantial effect on the electrochemical activity for methane oxidation. Optimal anode performance for methane oxidation has been obtained for $Sm_{0.2}(Ce_{0.83}Ti_{0.17})_{0.8}O_{1.9}$ (SCT0.17) modified Ni–YSZ anode with SCT0.17 loading of about 241 mg cm^{-2} resulted from four repeated impregnation cycles. When operating on humidified methane as fuel and ambient air as oxidant at 700 °C, single cells with the configuration of SCT0.17 modified Ni–YSZ anode, YSZ electrolyte and $La_{0.6}Sr_{0.4}Co_{0.2}Fe_{0.8}O_3$–$Sm_{0.2}Ce_{0.8}O_{1.9}$ (LSCF–SDC) composite cathode show the polarization cell resistance of 0.63 Ω cm^2 under open circuit conditions and produce a peak power density of 383 mW cm^{-2}. It has been revealed that the coated Ti-doped SDC on Ni–YSZ anode not only effectively prevents the methane fuel from directly impacting on the Ni particles, but also enhances the kinetics of methane oxidation due to an improved oxygen storage capacity (OSC) and redox equilibrium of the anode surface, resulting in significant enhancement of the SCT*x* modified Ni–YSZ anode for direct methane oxidation.

1. Introduction

Solid oxide fuel cells (SOFCs) have attracted great attention due to the high energy conversion efficiency and low emission, fuel flexibility and application versatility. The commercialization of the SOFC technology depends on the cell performance and the cost of the fuel cell system. It is advantageous if the SOFC anode can directly utilize widely available hydrocarbon fuels [1,2]. The conventional Ni-based anode exhibits excellent performance when H_2 is used as fuel, but fails at direct operation on hydrocarbon fuels due to carbon deposition (coking) issues, unless when substantial amount of H_2O, CO_2, or O_2 is present in the fuel (diluting fuel, reducing fuel efficiency and adding system cost), or when a cell is operated under some limited conditions (e.g. at $T < 700$ °C and high current density) [3,4]. However, Ni is such a powerful catalyst for breaking C–H bond that carbon formation can occur even when carbon is not the thermodynamically predicted product. Further, formation of nickel carbides can even cause the cell to fracture [5,6]. To prevent carbon formation in the anode for direct utilization of hydrocarbon fuels, an effective approach is to develop ceramic electronic or mixed ionic–electronic conducting anodes, such as $(La_{1-x}Sr_x)_{0.9}Cr_{0.5}Mn_{0.5}O_{3-\delta}$ (LSCM) [7], doped $SrTiO_3$ [8–11], and double-perovskite system $Sr_2Mg_{1-x}Mn_xMoO_{6-\delta}$ [12]. Unfortunately, these materials usually show very low electronic conductivity, making it difficulty in fabricating anode-supported cells. Park et al. reported Cu-ceria based anode for direct utilization of methane, ethane, 1-butene, *n*-butane or toluene fuels [13]. Although reasonable power densities have been achieved, one potential problem with Cu-based anodes is the sintering and agglomeration of Cu particles during cell operation at high temperatures due to the relatively low melting point (1085 °C) of copper [14]. Zhan and Barnett have reported that introduction of a Ru-ceria based reforming catalyst layer on top of the Ni-based anode for reforming hydrocarbon fuels to H_2 and CO before reaching the anode can achieve a stable output power density without anode coking [15,16]. However, the used precious metal can potentially make this method unpractical.

In principle, SOFCs are capable of operation directly on hydrocarbon fuels if the surface of the anode is supplied with sufficient oxygen for fuel oxidation and the anode kinetics is effectively enhanced as well. The conventional Ni–YSZ anode possesses many advantages such as low cost, high electronic and reasonable ionic

* Corresponding author. Tel.: +86 551 3601700; fax: +86 551 3607627.
E-mail address: jfgao@ustc.edu.cn (J. Gao).

0378-7753/$ – see front matter © 2011 Elsevier B.V. All rights reserved.
doi:10.1016/j.jpowsour.2011.01.062

conductivity, high stability in reducing atmospheres at high temperatures and moderate thermal expansion coefficient matching with the YSZ electrolyte. Most importantly, Ni and YSZ are essentially immiscible in each other and non-reactive over a very wide temperature range, enabling the cost-effective fabrication of a NiO–YSZ composite anode via conventional sintering followed by reduction upon exposure to fuel gases. Consequently, Ni–YSZ anode is always the preferred choice for SOFCs for practical applications. To solve the problem of carbon deposition, an effective strategy is to prevent hydrocarbon fuel from directly impacting on the surface of Ni particles and improve the anode kinetics of the fuel oxidation by coating the Ni–YSZ anode with catalytically active component such as nanosized ceria-based material [17].

The fluorite-type ceria has a good oxygen storage capacity (OSC) due to its well-known redox-property (Ce^{4+}–Ce^{3+}) [18]. Moreover, the OSC and redox equilibrium would be significantly enhanced by doping technique, such as doping with titanium or zirconium [19–22]. In this study, titania doped $Sm_{0.2}Ce_{0.8}O_{1.9}$ ($Sm_{0.2}(Ce_{1-x}Ti_x)_{0.8}O_{1.9}$, SCT*x*, x = 0–0.29) are explored to modify Ni–YSZ anode for direct utilization of methane fuel.

2. Experimental

2.1. SCTx synthesis and characterization

SCT*x* powders were synthesized by a glycine–nitrate process [23] and used for crystalline structure and redox-property characterization. Stoichiometric amount of SCT*x* from 1 mol aqueous solution of $Sm(NO_3)_3$, $Ce(NO_3)_3$ and $TiO(NO_3)_2$ was heated on a hot plate until combustion. The ash was then pulverized and calcined at 800 °C for 2 h to remove carbon residue. The final powders of SCT*x* with x = 0, 0.05, 0.10, 0.13, 0.17, 0.20, 0.23, 0.26, 0.29 and 0.33 were denoted as SCT0 (SDC), SCT0.05, SCT0.10, SCT0.13, SCT0.17, SCT0.20, SCT0.23, SCT0.26, SCT0.29 and SCT0.33, respectively. The crystalline structure of different SCT*x* was studied by X-ray diffraction (XRD) analysis over the 2θ range of 20–80° with a scanning rate of 1 °C min^{-1} on Scintag-I XRD instrument equipped with Cu-Kα radiation. The oxygen storage capacity and redox behavior were examined by temperature programmed reduction (TPR).

2.2. Single cell preparation and surface modification of Ni–YSZ anode

Tubular single cells with an effective area of 1.0 cm^2 consisting of 1 mm thick porous Ni–YSZ anode support prepared by gel casting, ~5 μm fine Ni/YSZ anode interlayer and ~20 μm YSZ electrolyte (Tosoh, TZ-8YSZ) by slurry-coating/co-sintering technique, and $La_{0.6}Sr_{0.4}Co_{0.2}Fe_{0.8}O_3$-$Sm_{0.2}Ce_{0.8}O_{1.9}$ (LSCF–SDC) composite cathode (with the weight ratio of LSCF:SDC = 6:4) by screen-printing were used in this study. Commercial NiO (Lanzhou Jinchuan Metal Material Technology Co., China) and YSZ (Farmeiya Advanced Materials Co., China) were used as the starting powders for the anode support preparation. The fine NiO–YSZ powders for the fabrication of the anode interlayer were synthesized by a co-precipitation technique. LSCF powder was synthesized by a glycine–nitrate process. SDC power was synthesized by the oxalate coprecipitation technique [24]. The detailed cell fabrication procedures can be found in our previous publication [17].

The porous NiO–YSZ anode support (before reduction) of the single cells was impregnated using 1 mol aqueous solution of $Sm(NO_3)_3$, $Ce(NO_3)_3$ and $TiO(NO_3)_2$, followed by drying in an oven at 60 °C for 12 h and firing at 800 °C, resulting in a coated layer of $Sm_{0.2}(Ce_{1-x}Ti_x)_{0.8}O_{1.9}$ (SCT*x*, x = 0–0.29) nano-particles on the surfaces of NiO–YSZ anode support. This cycle was repeated until a desirable SCT*x* loading level was achieved. The SCT*x* loading level was determined by the weight difference before and after each impregnation treatment cycle.

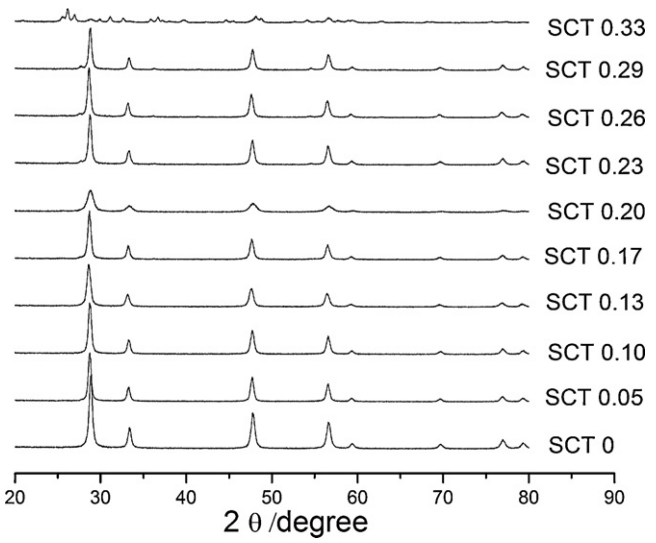

Fig. 1. XRD patterns of SCT*x* (x = 0–0.33).

2.3. Cell testing

Cell testing was carried out using a setup consisting of a program controlled electric furnace and a cell holder made of two alumina tubes, digital multimeters (HP CDM-8145) and an electrochemical workstation (Zahner IM6e). The cell was first sandwiched between two alumina tubes (the cell holder) and sealed with silver paste (DAD-87, Shanghai Research Institute of Synthetic Resins). Silver wires were used as the lead wires for both the anode and the cathode. Prior to the cell electrochemical performance testing, the NiO–YSZ anode was reduced to Ni–YSZ under flowing H_2. Humidified (3 vol% H_2O) methane or H_2 was used as fuel and ambient air as oxidant. The impedance spectra of the cells were measured under open-circuit conditions over a frequency range from 0.1 Hz to 1 MHz. The cell polarization resistance (R_p) was determined from the difference between the low and high frequency intercepts of the impedance spectra with the real axis in the Nyquist plot. The short-time stability of the cells using CH_4 as fuel was examined under a constant cell voltage of 0.50 V at 700 °C. The cell microstructure was characterized using a scanning electron microscope (SEM, JSM-6700F, JEOL).

3. Result and discussion

3.1. Crystalline structures and redox behaviors of SCTx

Shown in Fig. 1 are the XRD patterns of SCT*x* with x = 0–0.33. It can be seen that single phase fluorite-type cubic structure can be obtained when $x \leq 0.29$. The lattice parameter decreases from 5.41 to 5.39 Å with an increase in x from 0 to 0.29 since the ion size of Ti^{4+} (0.68 Å) is smaller than that of Ce^{4+} (1.01 Å). In addition, SCT*x* particle growth during calcination process is suppressed by substitution of Ce^{4+} with Ti^{4+}, as revealed from the broadening XRD peaks with the increase in the concentration of the Ti-doping. However, when the Ti-doping is higher than 0.29 (x = 0.33), secondary phases (a mixture of anatase and rutile TiO_2) appear. These results are in agreement with the previous reports [25,26].

Fig. 2 shows the H_2-TPR profiles of different SCT*x* (x = 0–0.29) and TiO_2. The samples were first pretreated with pure N_2 at 400 °C for 1 h with a ramping rate of 10 °C min^{-1} and then cooled in the

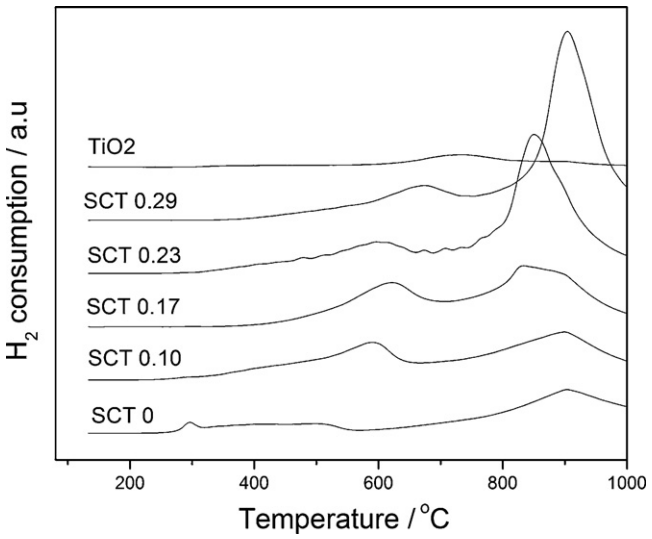

Fig. 2. H_2-TPR profiles of SCTx (x = 0–0.29) and TiO_2.

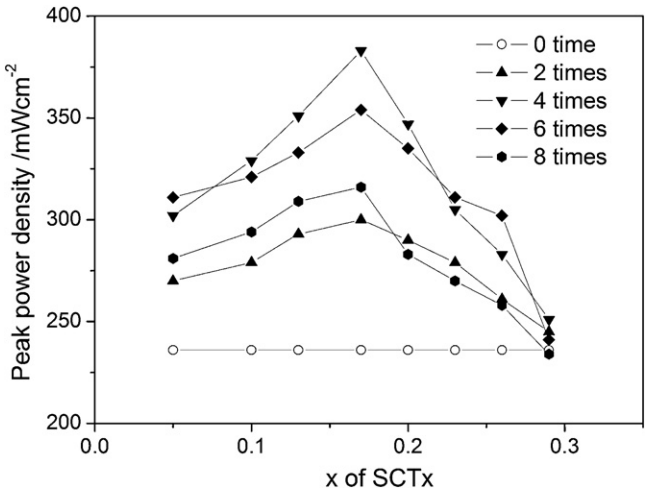

Fig. 3. Peak power densities of the cells with anodes modified with different Ti-doping and impregnation cycles tested at 700 °C using H_2 as fuel and air as oxidant.

quartz tube reactor. The TPR was conducted using a gas chromatograph equipped with a thermal conductivity detector with a flow of 5% H_2 in N_2 as the reducing agent over a temperature range from 80 to 1000 °C and a scanning rate of 10 °C min^{-1}. There are two peaks for each of the SCTx samples. The first peak starts at about 300 °C and is generally considered to be associated with the reduction of the SCTx solid solution surface. The second peak appears at a higher temperature and is usually related to the SCTx solid solution bulk reduction [27]. It can be seen that the H_2 consumption associated with the surface reduction, which is more important for the fuel oxidation of an anode, increases with the increase in Ti-doping concentration, reaches the maximum for SCT0.17, and then decreases with further increase in Ti-doping. The overall H_2 consumption (the sum of the surface and bulk reduction) increases with the Ti-doping content in SCTx for the solutions with x = 0–0.29. This is usually explained as distortion of the fluorite-type structure due to Ti-doping [28].

3.2. Effects of Ti-doping content and the loading of SCTx on the anode electrochemical performance

The unreduced NiO–YSZ anode support has an open porosity of about 29% and a thickness of 1 mm. The NiO–YSZ anode support was impregnated with aqueous solution of SCTx, dried in an oven at 60 °C for 12 h and fired at 800 °C for 2 h. The impregnation cycle was repeated until a desirable SCTx loading was achieved. Fig. 3 shows the peak power densities of the cells with anodes modified with different Ti-doping level and various impregnation cycles tested at 700 °C using H_2 as fuel and air as oxidant. Results show that Ti-doping has lead to a significant enhancement of the cell power output. Further, it can be seen that the electrochemical performance of the Ni–YSZ anode modified with different SCTx increases with the increase in Ti-doping concentration, reaches the maximum for x = 0.17, and then decreases with further increase in the concentration of Ti-doping, consistent with the TPR results, implying that the enhancement of the cell performance is due to improvement in the anode surface reduction. It has also been found that cells with the NiO–YSZ anode modified after 4 impregnation cycles have the most cell performance enhancement when the anodes are modified with different SCTx. Among the different Ti-doping concentration, x = 0.17 shows the highest cell performance improvement. The best cell performance was obtained for the cells with anode modified with SCT0.17 (x = 0.17) and 4 impregnation cycles (resulting in the SCT0.17 loading of ~241 mg cm^{-2}).

The SCTx loading level on the NiO–YSZ anode has substantial impact on the cell performance for different SCTx. A low SCTx loading, consequently a thin coating of SCTx might result in an insufficient improvement of the anode electrochemical activity while an excessive SCTx loading can lead to a reduced porosity and consequently an increased resistance for the diffusion of the fuel. The improvement varies with different SCTx suggests that the oxygen storage capacity and redox behavior of SCTx are closely related to the Ti-doping content in SCTx. As a comparison, Table 1 lists the peak power densities and the polarization resistances (R_p) of the cells of which the NiO–YSZ anode was modified with SDC (C-SDC) and SCT0.17 (C-SCT17) after 4 impregnation cycles, respectively, and of the cell with an unmodified Ni–YSZ anode (Cell-0), operating with H_2 as fuel and air as oxidant. Under the same experimental conditions, the performance of C-SCT17 is higher than that of C-SDC and much higher than that of Cell-0.

3.3. Cell performance

Fig. 4 shows the cell voltage, current and power output curves of C-SCT17 and C-SDC with either CH_4 or H_2 as fuel and air as oxidant operated at 700 °C. It can be seen that C-SCT17 has better cell performance than that of C-SDC using CH_4 as fuel, indicating that the Ni–YSZ anode modified with SCT0.17 has higher electrochemical activity for CH_4 oxidation than that of the anode modified

Table 1
The peak power densities and ASR of the cells with the Ni–YSZ anodes modified by SCD and SCT0.17 after 4 times impregnation cycle, respectively, and with an unmodified Ni–YSZ anodes.

Cell	P_{max} (mW cm^{-2})			R_p (Ω cm^2)		
	700 °C	750 °C	800 °C	700 °C	750 °C	800 °C
C-SDC	336	463	537	0.71	0.28	0.15
C-SCT17	383	487	565	0.63	0.21	0.10
Cell-0	236	359	486	1.69	0.99	0.36

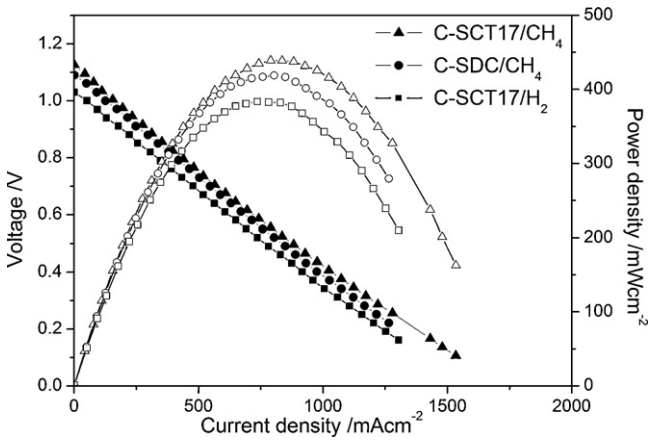

Fig. 4. *I-V-P* curves of C-SCT17 and C-SDC using CH_4 or H_2 as fuel at 700 °C.

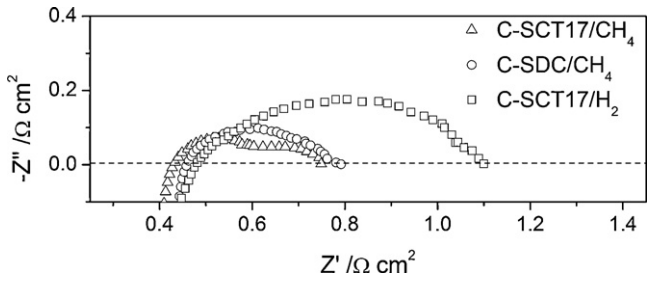

Fig. 5. Impedance spectra of the cell C-SCT17 and C-SDC as using CH_4 or H_2 as fuel under open circuit conditions.

with SDC. Consequently, it seems that Ti-doping in SDC results in an improved oxygen storage capacity and/or a rapid redox-equilibrium of SCT0.17, as demonstrated in the TPR results shown in Fig. 2. Further, the Ni–YSZ anode modified with SCT0.17 shows a higher electrochemical activity for CH_4 oxidation than that for H_2.

Shown in Fig. 5 are the impedance spectra of C-SCT17 and C-SDC with either CH_4 or H_2 as fuel and air as oxidant operated at 700 °C under open circuit conditions. When CH_4 is used as fuel, the overall cell interfacial resistance, R_p of C-SCT17 is about 0.31 Ω cm^2, a little bit lower than that of C-SDC, which is 0.32 Ω cm^2 at the same testing condition. However, C-SCT17 shows a much higher R_p of 0.63 Ω cm^2 when using H_2 as fuel. This is in agreement with the above cell power output results.

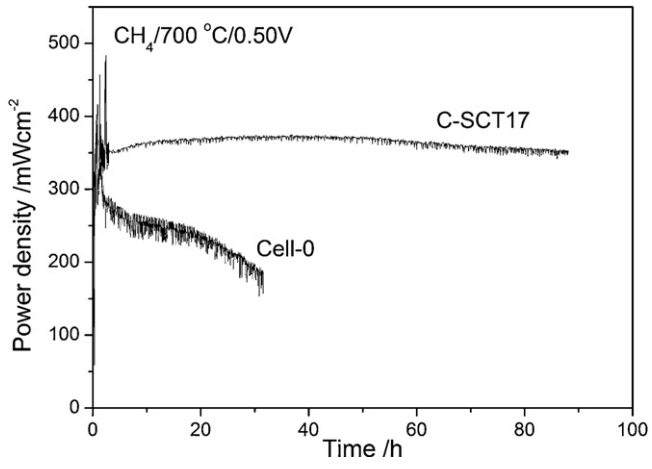

Fig. 6. The short-term stabilities of C-SCT17 and Cell-0 under a constant voltage of 0.50 V tested at 700 °C using humidified methane as fuel.

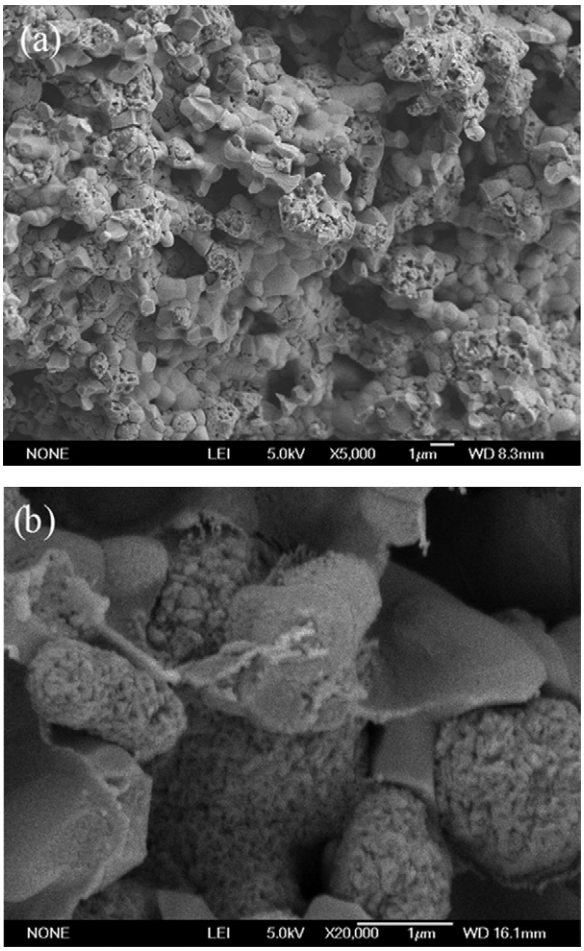

Fig. 7. SEM images of the unmodified Ni–YSZ anode (a) and the anode of Ni–YSZ modified with SCT0.17 (b).

Fig. 6 shows the short-term stability test of C-SCT17 and Cell-0 under a constant cell voltage of 0.50 V at 700 °C using humidified methane (3% H_2O) as fuel. The cell C-SCT17 shows an acceptable cell performance stability in the testing period, but the cell with the unmodified Ni–YSZ anode (Cell-0) degrades rapidly with time.

Shown in Fig. 7 are the SEM images of the unmodified Ni–YSZ anode and the Ni–YSZ anode modified with SCT0.17 after 4 impregnation cycles. For the unmodified anode, the surface of Ni particle is fully exposed. As for the modified anode, both the surfaces of Ni and YSZ particles are coated with a thin layer of nano-sized SCT0.17. Consequently, CH_4 molecules would be prevented from directly impacting on the Ni particles by the coated SCT0.17 layer and carbon deposition on the Ni surface would be avoided accordingly due to the catalytic cracking of C–H. Further, SCT0.17 would provide catalytic activity to reform CH_4.

4. Conclusions

The conventional Ni–YSZ anode has been modified with Ti-doped SDC (SCT*x*, *x* = 0–0.29) by ion-impregnation and used for direct utilization of methane fuel. Both the Ti-doping content in SDC and the loading level of SCT*x* have shown substantial impact on the electrochemical performance of the resulted anodes. The anode modified with SCT0.17 with a loading of 241 mg cm^{-2} after 4 impregnation cycles shows the most improved performance. Cells with the optimized anode demonstrate peak power density of 444 mW cm^{-2} and show reasonably stable cell performance using methane as fuel and air as oxidant at 700 °C. The coated nano-

sized SCT0.17 layer on the Ni surface effectively prevents methane from directly impacting on the Ni particle and enhances the oxygen storage and redox behavior of the anode, consequently improving the oxygen supply for methane oxidation and suppressing carbon deposition, and resulting in a significant performance enhancement of the modified anode. Results show that the conventional Ni-based anode can be modified by SCT0.17 impregnation and used for direct methane fuel cells.

Acknowledgements

This work was financially supported by the National Natural Science Foundation of China (20871110), Anhui Science and Technology Department (08010202126) and the US National Science Foundation (CBET 0967166).

References

[1] R.J. Gorte, J.M. Vohs, S. McIntosh, Solid State Ionics 175 (2004) 1–6.
[2] A. Atkinson, S. Barnett, R.J. Gorte, J.T.S. Irvine, A.J. McEvoy, M. Mogensen, S.C. Singhal, J. Vohs, Nat. Mater. 3 (2004) 17–27.
[3] C. Lu, S. An, W.L. Worrell, J.M. Vohs, R.J. Gorte, Solid State Ionics 175 (2004) 47–50.
[4] Y.B. Lin, Z.L. Zhan, S.A. Barnett, J. Power Sources 158 (2006) 1313–1316.
[5] X. Wang, R.J. Gorte, Catal. Lett. 73 (2001) 15–19.
[6] G. Bae, J. Bae, P. Kim-Lohsoontorn, J. Jeong, Int. J. Hydrogen Energy 35 (2010) 12346–12358.
[7] S. Tao, J.T.S. Irvine, Nat. Mater. 2 (2003) 320–323.
[8] S. Hui, A. Petric, J. Eur. Ceram. Soc. 22 (2002) 1673–1681.
[9] M.R. Pillai, I. Kim, D.M. Bierschenk, S.A. Barnett, J. Power Sources 185 (2008) 1086–1093.
[10] H. Zhao, F. Gao, X. Li, C. Zhang, Y. Zhao, Solid State Ionics 180 (2009) 193–197.
[11] H. Kurokawa, L. Yang, C.P. Jacobson, L.C. De Jonghe, S.J. Visco, J. Power Sources 164 (2007) 510–518.
[12] Y.H. Huang, R.I. Dass, Z.L. Xing, J.B. Goodenough, Science 312 (2006) 254–257.
[13] S. Park, J.M. Vohs, R.J. Gorte, Nature 404 (2000) 265–267.
[14] S. Tao, J.T.S. Irvine, Chem. Rec. 4 (2004) 83–95.
[15] Z. Zhan, S.A. Barnett, Science 308 (2005) 844–847.
[16] Z. Zhan, S.A. Barnett, Solid State Ionics 176 (2005) 871–879.
[17] L. Zhang, J. Gao, M. Liu, C. Xia, J. Alloys Compd. 482 (2009) 168–172.
[18] J. Kaspar, P. Fornasiero, M. Graziani, Catal. Today 50 (1999) 285–298.
[19] E. Mamontov, T. Egami, J. Phys. Chem. Solids 61 (2000) 1345–1356.
[20] J. Rynkowski, J. Farbotko, R. Touroude, L. Hilaire, Appl. Catal. A: Gen. 203 (2000) 335–348.
[21] S. Pengpanich, V. Meeyoo, T. Rirksomboon, Catal. Today 93–95 (2004) 95–105.
[22] T. López, F. Rojas, R. Alexander-Katz, F. Galindo, A. Balankin, A. Buljan, J. Solid State Chem. 177 (2004) 1873–1885.
[23] L.A. Chick, L.R. Pederson, G.D. Maupin, J.L. Bates, L.E. Thomas, G.J. Exarhos, Mater. Lett. 10 (1990) 6–12.
[24] R. Peng, C. Xia, D. Peng, G. Meng, Mater. Lett. 58 (2004) 604–608.
[25] S. Watanabe, X. Ma, C. Song, J. Phys. Chem. C 113 (2009) 14249–14257.
[26] G.W. Lee, J.H. Byeon, Mater. Charact. 60 (2009) 1476–1481.
[27] H.C. Yao, Y.F.Y. Yao, J. Catal. 86 (1984) 254–265.
[28] G. Dutta, U.V. Waghmare, T. Baidya, M.S. Hegde, K.R. Priolkar, P.R. Sarode, Chem. Mater. 18 (2006) 3249–3256.